A Highly Efficient Synthetic Vector: Nonhydrodynamic Delivery of DNA to Hepatocyte Nuclei *in Vivo*

Yunxia Hu,[‡,*] Matthew T. Haynes, Yuhua Wang, Feng Liu, and Leaf Huang[*]

The Center for Nanotechnology in Drug Delivery, Division of Molecular Pharmaceutics, Eshelman School of Pharmacy, The University of North Carolina at Chapel Hill, Chapel Hill, North Carolina 27599, United States. [‡]Present address: Yantai Institute of Coastal Zone Research, Chinese Academy of Sciences, Seventeen ChunHui Road, Laishan District, Yantai, Shandong, China 264003.

ABSTRACT Multifunctional membrane-core nanoparticles, composed of calcium phosphate cores, arginine-rich peptides, cationic and PEGylated lipid membranes, and galactose targeting ligands, have been developed as synthetic vectors for efficient nuclear delivery of plasmid DNA and subsequent gene expression in hepatocytes *in vivo*. Targeted particles exhibited rapid and extensive hepatic accumulation and were predominantly internalized by hepatocytes, while the inclusion of such peptides in LCP was sufficient to elicit high degrees of nuclear translocation of plasmid DNA. Monocyclic CR8C significantly enhanced *in vivo* gene expression over 10-fold more than linear CR8C, likely due to a release-favoring mechanism of the DNA/peptide complex. Though 100-fold lower in activity than that achieved *via* hydrodynamic injection, this formulation presents as a much less invasive alternative. To our knowledge, this is the most effective synthetic vector for liver gene transfer.

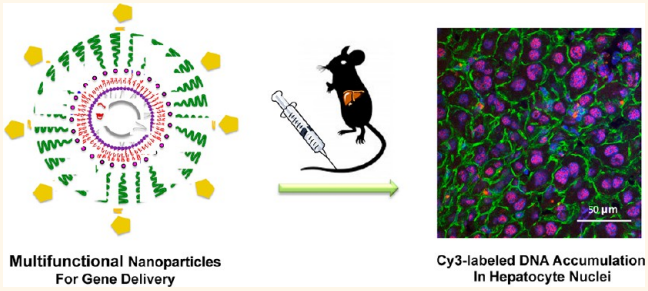

KEYWORDS: nanoparticle · liposome · liver · hepatocyte · DNA delivery · arginine-rich peptide

Despite significant advantages in loading, targeting, and safety, among others, provided by synthetic vectors for gene delivery, they still do not compare well with viral vectors in terms of delivery efficiency.[1−5] A variety of polymeric,[6−8] liposomal,[9,10] protein-based,[11,12] organic,[13,14] and inorganic[15,16] materials have been developed to incorporate certain viral characteristics, and vector platforms which can cohesively integrate multiple functionalities present the greatest potential utility.[17] The needs in artificial virus development for DNA delivery have been outlined previously;[3] briefly, therapeutic loading, stability and longevity in vascular transit, distribution to and uptake into the cells of interest, endosomal escape, intracellular trafficking, nuclear import, and transcriptional promotion and lifespan must be rationally considered in effective vector design.

The hepatocytes of the liver present as desirable gene therapy targets for a variety of disease states,[5,18] including Wilson Disease,[19] α1-Antitrypsin Deficiency,[20] viral hepatitis,[5] and Factor VII Deficiency,[21] primarily due to systemic accessibility, the highly endocytic nature of hepatocytes, and the potential for high degrees of tissue exposure based on organ physiology.[5] The hepatic sinusoidal epithelium acts as the primary structural and functional barrier to hepatocyte exposure, with fenestrations (numbering $8.7 \pm 0.5/\mu m^2$ with an average diameter of 141 ± 10.8 nm in C57BL/6 mice) patrolled by a large population of resident immune cells (*e.g.*, Kupffer cells).[22,23] Typically, formulations employ a dense coating of antifouling agents such as polyethylene glycol (PEG) to both increase circulation longevity and limit alternative cell uptake, as well as active targeting strategies to promote uptake by hepatocytes; sugars such as galactose[24,25] and *N*-acetylgalactosamine[8] have been studied extensively in this regard for uptake *via* the asialoglycoprotein receptor (ASGPR).

Upon internalization into endosomes, the contents of the delivery vehicle must escape to avoid lysosomal sequestration,

* Address correspondence to yunxiahu@yic.ac.cn, leafh@unc.edu.

Received for review March 11, 2013 and accepted May 6, 2013.

Published online May 06, 2013
10.1021/nn4012384

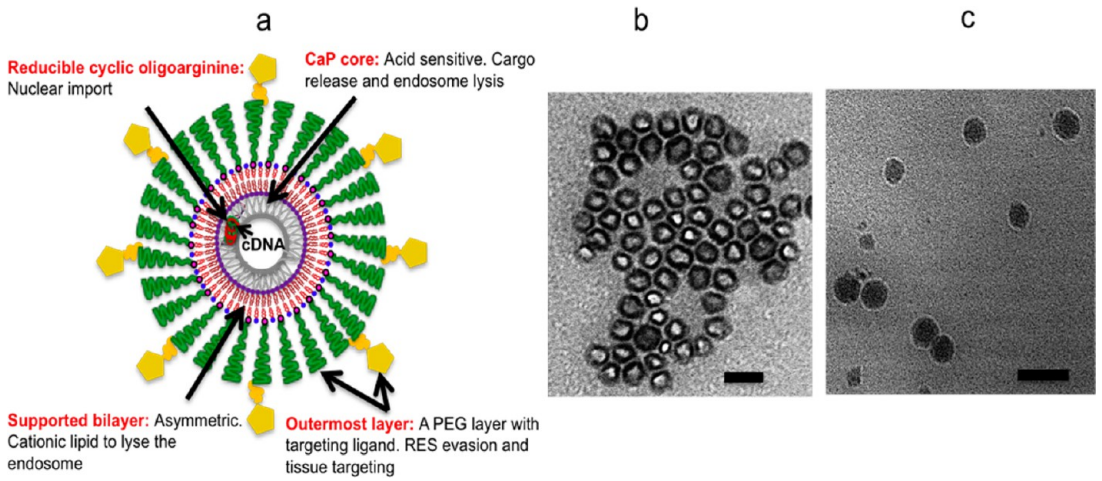

Figure 1. (a) Representative multifunctional features of membrane-core LCPs consist of calcium phosphate cores encapsulating DNA and octaarginine peptides, and an asymmetric lipid membrane functionalized with galactose ligands on a stealth PEG layer. (b) TEM image of LCP cores loaded with DNA and octaarginine peptides (scale bar: 50 nm). (c) TEM image of final LCPs, stained with uranyl acetate (scale bar: 100 nm).

TABLE 1. Size and Zeta Potential of PEGylated LCP

	size (d, nm)	potential (mV)	PDI
LCP-DNA-Gal[a]	52 ± 8	5 ± 2	0.18
LCP-(DNA+ mc-CR8C)-Gal[a]	57 ± 10	10 ± 3	0.24
LCP-(DNA+ l-CR8C)-Gal[a]	56 ± 11	8 ± 3	0.23

[a] Gal, galactose; mc, monocyclic; l, linear.

a process typically achieved by buffering-induced osmotic bursting,[26] cationic lipid-mediated ion-pair formation,[27] or various other endosomolytic molecules.[10,28] After release, however, trafficking to the nucleus and nuclear import must still be mediated. Interest has been shown in a variety of oligopeptide species employing high densities of cationic charge (lysine,[29] arginine,[30,31] and histidine[32] residues), either alone or in concert with nuclear localization sequences, to support nuclear translocation; specifically, arginine-rich bioreducible polymers and polypeptides have been explored *in vitro*[29,30] and *in vivo*[17,33] as efficacious and nontoxic transfection systems. However, extensive vesicular entrapment of arginine-rich materials has been suggested as the primary inefficiency of their use in DNA delivery.[34]

With such studies in mind, we have developed membrane-core nanoparticles (LCP, Liposome Calcium Phosphate) inspired by rational design, integrating calcium phosphate nanoprecipitate (CaP) cores, cysteine-flanked octaarginine peptides (Cys-$(Arg)_8$-Cys, CR8C; Supporting Information Figure s1), and asymmetric lipid membranes[35] (densely coated with PEG and targeted *via* galactose ligands) together to achieve surprising levels of gene expression within hepatocytes *in vivo* through intravenous injection in a non-hydrodynamic manner. Targeted LCP distributed rapidly and extensively to the liver and was predominantly internalized by hepatocytes, while the inclusion

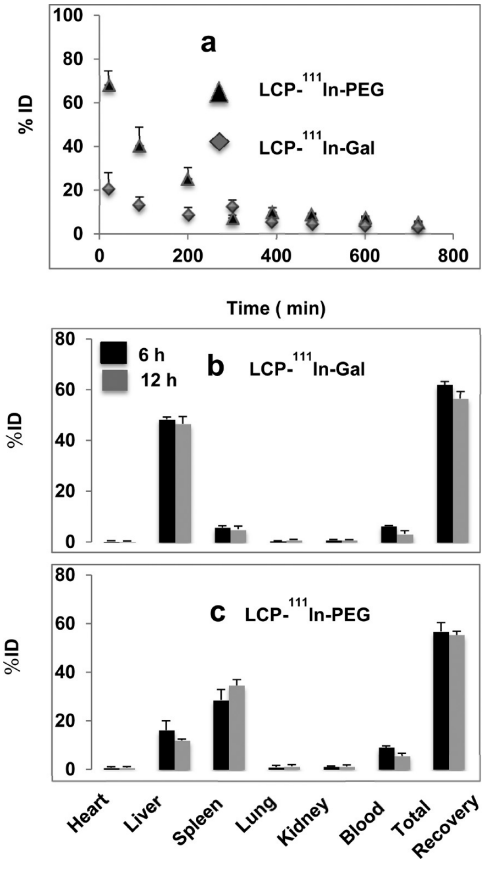

Figure 2. (a) Serum kinetics and (b and c) biodistribution of LCP loaded with luciferase DNA and mc-CR8C (with or without galactose) in which LCP was labeled with ^{111}In.

of such peptides in LCP was sufficient to promote high degrees of nuclear translocation and expression of plasmid DNA. Interestingly, co-delivery with monocyclic CR8C significantly enhanced *in vivo* gene expression over 10-fold more than linear CR8C, possibly due to differences in the degree of peptide-DNA

condensation and dissociation upon release. Based on our exploration of the current literature, our formulation presents as the most effective synthetic vector for liver gene transfer.

RESULTS AND DISCUSSION

Representative multifunctional features of the membrane-core LCP structures are shown in Figure 1a. A reverse microemulsion established by a strong surfactant (IGEPAL-520) is utilized to prepare small, 1,2-dioleoyl-*sn*-glycero-3-phosphate (DOPA)-coated CaP nanoparticles (LCP "cores") which can encapsulate both DNA (appx. 50% efficiency) and peptides, with core size ranging from 20 to 30 nm in diameter.[35] The hollow core structure can be visualized under Transmission Electron Microscopy (TEM) (Figure 1b). Further, the DOPA monolayer surrounding the CaP core allows for the confined assembly of outer leaflet lipids (1,2-dioleoyl-3-trimethylammonium-propane (DOTAP), cholesterol, 1,2-distearoyl-*sn*-glycero-3-phosphatidylethanolamine-*N*-[succinyl(polyethylene glycol)-2000 (DSPE-PEG_{2000})), producing sub-100 nm particles ("final" LCP, 40−60 nm in diameter, shown in Figure 1c) which can easily penetrate hepatic sinusoidal fenestrations.

TABLE 2. Kinetic Analysis Based on Recovery of LCP-Associated ^{111}In Radioactivity[a]

kinetic analysis	Cl_{dist} (mL/h)	V_{blood} (mL)	$t_{1/2}^{dist}$ (h)	$t_{1/2}^{elim}$ (h)
LCP-Gal	4.71 ± 0.22	4.16 ± 0.04	0.61	6.80
LCP-PEG	0.35 ± 0.15	1.24 ± 0.06	2.46	5.78

[a] Data are reported as estimate ± standard error. CL_{dist} = distribution clearance; V_{blood} = volume of distribution in the circulation compartment; $t_{1/2}^{dist}$ = distribution-phase half-life (estimated as $Ln(2)V_{blood}/CL_{dist}$, assuming unidirectional initial distribution from the circulation compartment to the peripheral compartment [*i.e.* liver and/or spleen]); $t_{1/2}^{elim}$ = elimination-phase half-life (estimated from a linearization of the terminal phase kinetic profile).

PEGylation of LCP was confirmed by a fluorescence method, in separation from micelles *via* sucrose gradient centrifugation, to be 20 mol % of outer leaflet lipids (data not shown). The hydrodynamic diameter and the surface charge of the LCP particles are outlined in Table 1. Dynamic light scattering indicated that LCP was narrowly dispersed around 55 nm in diameter, with a near-neutral zeta potential (around +9 mV) due to charge shielding by PEGylation.

LCP was radiolabeled with ^{111}In during the preparation of CaP core in a similar manner to previously published methods[36] and intravenously injected into C57BL/6 female mice to examine its distribution *in vivo*. Quantitative pharmacokinetic and biodistribution analyses of ^{111}In-labeled LCP indicated that galactose-targeted LCP distributed rapidly and primarily to the liver (Figure 2 and Table 2), with 48 ± 1% injected dose (ID) recovered in the liver at 6 h post-injection. In comparison, 16 ± 4% and 29 ± 4% ID were recovered 6 h post-injection in the liver and the spleen, respectively, in mice treated with untargeted LCP. Targeting *via* galactose likely altered the LCP distribution profile due to increased uptake through ASGPR-mediated endocytosis, as opposed to relying upon cationic lipid-mediated cellular interactions facilitated by PEGy-lation shedding from LCP in the circulation.[37] Such a perspective is supported by the increased (3-fold) degree of liver distribution, decreased (4-fold) distribution half-life, and increased *in vitro* hepatocyte uptake (Table 2) associated with the galactosylated particles.

The synergistic function of the cationic lipids and the acid-sensitive CaP in the lysis of the endosome has been described previously for LCP,[35] however, effective nuclear import still presents as a significant challenge toward establishing efficacy, especially in non-proliferative cells such as hepatocytes. Viral vectors

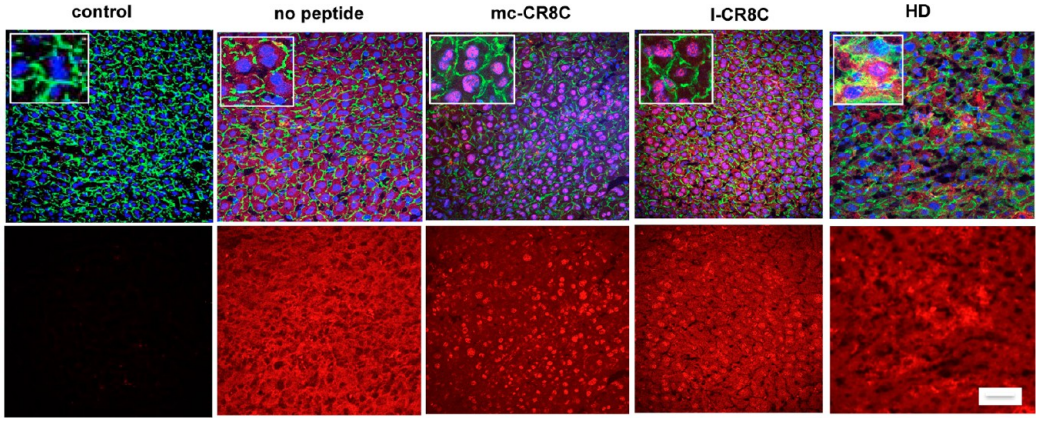

Figure 3. Intracellular Cy3-DNA fluorescence distribution in cryo-sections of liver tissues from C57BL/6 mice treated with LCP-(Control DNA)-Gal, LCP-(Cy3-DNA)-Gal, LCP-(Cy3-DNA+mc-CR8C)-Gal, LCP-(Cy3-DNA+l-CR8C)-Gal, and hydrodynamic (HD) injection 6 h after injection. Top images are fluorescence overlay of red from Cy3-DNA, blue from DAPI-stained nuclei, and green from FITC-labeled Phalloidin-stained actin; bottom images are Cy3-DNA fluorescence only. Inset images are an increased magnification, to better illustrate intranuclear Cy3-DNA fluorescence. Monocyclic abbreviated to mc, linear abbreviated to l. Scale bar: 25 μm.

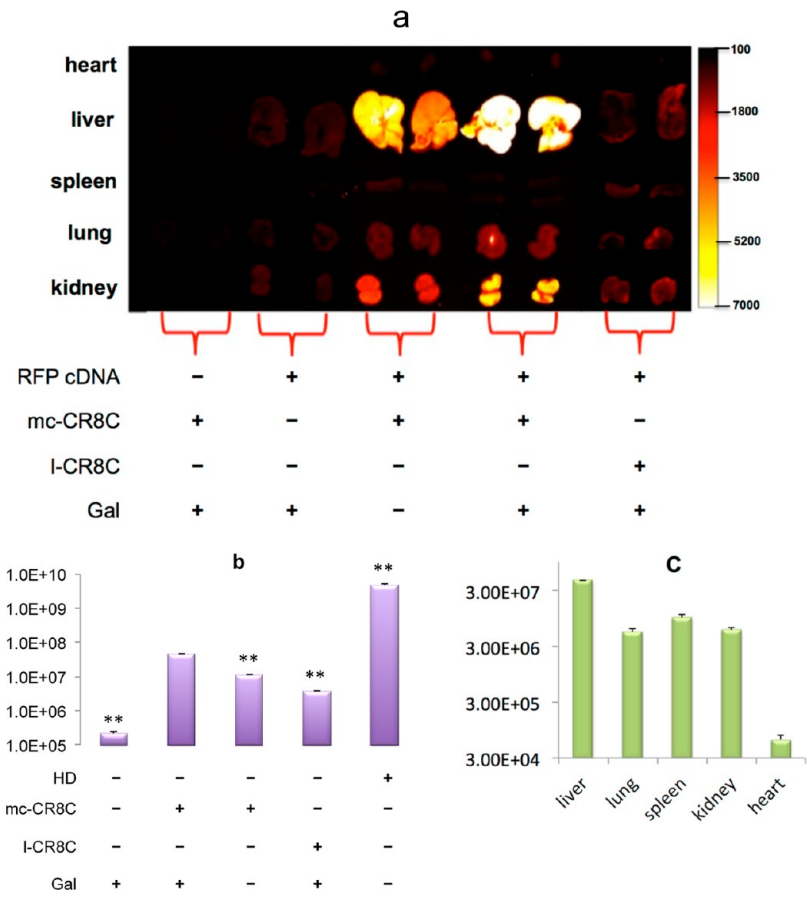

Figure 4. Transgene expression in the major organs of C57BL/6 mice 24 h after intravenous injection of plasmid formulated in different groups of LCP (plasmid dose: 0.3 mg/kg). (a) Comparison of expressed RFP fluorescence, as determined with a Kodak IVIS system (ex/em: 550/600 nm). Control DNA was a luciferase plasmid. (b) Comparison of expressed luciferase in the liver. All are compared with the group of Gal-targeted LCP containing mc-CR8C. $N = 3$ per group. **: $p < 0.0125$. (c) Comparison of expressed luciferase in various major organs after the administration of plasmid formulated in the Gal-targeted LCP containing mc-CR8C.

typically employ nuclear localization sequences (NLS) for translocation of genetic material, which are readily recognized by the cellular nuclear transport machinery.[38] In terms of cellular uptake, octaarginine mimics the NLS of the HIV-1 Tat protein (Tat-(48−60));[10,39−41] however, on a postendosomal basis, its utility has not been fully characterized. In order to examine their effects on the intracellular distribution of the delivered DNA in the liver, Cy3-labeled DNA was encapsulated in different formulations of LCP (with linear CR8C (l-CR8C), with monocyclic CR8C (mc-CR8C), or without CR8C) and intravenously injected into C57BL/6 female mice. Livers were harvested 6 h postadministration, and their cryo-sections were observed by confocal microscopy after staining actin and nuclei. LCP encapsulating no CR8C was taken up into most of the hepatocytes in the liver; however, the majority of the Cy3-DNA distributed homogeneously in the cytoplasm (Figure 3). Co-encapsulation with either mc-CR8C or l-CR8C elicited extensive Cy3-DNA distribution to the hepatocyte nuclei, strongly suggesting that the arginine-rich peptides could mediate delivery of DNA into the nucleus. *In vitro* study further supported the efficient nuclear delivery of Cy3-DNA by coencapsulation with such peptides in LCP, with more than 90% of nuclei presenting strong Cy3 fluorescence (Supporting Information Figure s3). Such extensive uptake into hepatocytes *in vivo* is likely supported in part by effective mononuclear phagocyte evasion as well; our lab has recently shown extensive evasion of Kupffer cell uptake by LCP at higher densities of outer leaflet lipid PEGylation (greater than 10−15 mol %).[42] The most powerful nonviral method, hydrodynamic (HD) injection,[43] was used as a positive control to deliver Cy3-DNA to the liver. Fluorescence was observed in this case to be punctate and largely confined to the cytoplasm, with a minor amount accumulating in hepatocyte nuclei.

Plasmids encoding tdTomato red fluorescence protein (RFP) or firefly luciferase (Luc) driven by the cytomegalovirus promoter were then used, respectively, as semi-quantitative and quantitative reporter genes by which to characterize LCP as a vector in mice. Expression and activity were evaluated at 24 h postinjection, and analysis of major organs confirmed predominant hepatic transgene expression (Figure 4).

Interestingly, gene expression was relatively low in the spleen despite extensive accumulation of LCP on a % ID/gram basis; such particles likely possess limited ability to internalize into splenocytes. ASGPR-targeting of LCP *via* galactose proved effective in increasing both RFP and luciferase expression (Figure 4), as did targeted co-delivery with mc-CR8C peptide, which increased gene expression 200-fold over targeted LCP containing no peptide. Further, co-delivery with mc-CR8C both dramatically increased RFP expression and significantly increased luciferase expression (4.6×10^7 RLU/mg protein at a 0.3 mg DNA/kg dose) in the liver over l-CR8C. Since the two peptides were not observably different in supporting the nuclear import of plasmid DNA (Figure 3), such differences in reporter gene expression may involve differences in peptide-mediated plasmid condensation and release. It has been reported that excessive strength in DNA complexation by peptide-based condensing agents can both limit intracellular release and reduce overall efficacy,[44] often on structural and sequence-specific bases.[45] Likely supported by a greater conformational flexibility, l-CR8C more readily condensed plasmid DNA than mc-CR8C, as shown by an enhanced ability to exclude DNA-SYBR Green fluorescence (Figure 5a) and a more limited dissociation profile in the presence of anionic materials such as hyaluronan (Figure 5b). Further, the uneven fluorescence distribution in the nuclei (Figure 3) suggests that the DNA was still bound in rigid complexes, which could hinder DNA trafficking and transcription within the nuclei. Our HD comparator supports such a perspective as well; although HD injection delivers less DNA overall to the nuclei (Figure 3), all of such DNA would be free for transcription. Notably, our results present a step toward the outperformance of HD injection; though 100-fold lower in gene expression, our system presents a greatly decreased invasiveness in its application.

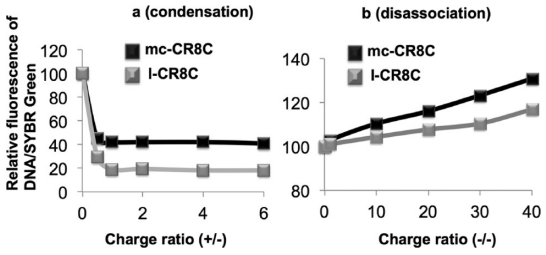

Figure 5. Condensation and decondensation of DNA/CR8C complexes. (a) Fluorescence quenching associated with the exclusion of DNA-SYBR Green by mc-CR8C and l-CR8C at different charge ratios (±, CR8C over DNA). (b) Fluorescence recovery through the dissociation of DNA-CR8C complexes driven by hyaluronic acid (HA) at different charge ratios (−/−, HA over DNA).

Our gene delivery system compares favorably against a variety of synthetic vectors on the basis of luciferase activity *in vivo*. For example, intratumoral injection of poly(amine-*co*-ester)-DNA complexes (0.5 mg DNA/kg) at best elicited luciferase activity on the order of 10^5 RLU/mg protein despite a simplified delivery process.[46] Hepatic luciferase activity of 7.5×10^5 RLU/mg protein was observed after intravenous administration of a galactose-conjugated bifunctional dendrimer (2.5 mg DNA/kg).[47] The optimal linear, cationic polymer from a small azide−alkyne click library supported gene expression in a subcutaneous tumor relative to 10^6 RLU/mg protein when dosing intravenously at 2 mg DNA/kg.[48] Alkylated (ethyl) polyethyleneimine (PEI) produced similar results as well in intravenous delivery to the lungs (2.5 mg DNA/kg).[49] One of the best direct comparisons, however, can be made to the pH-sensitive and octaarginine-modified

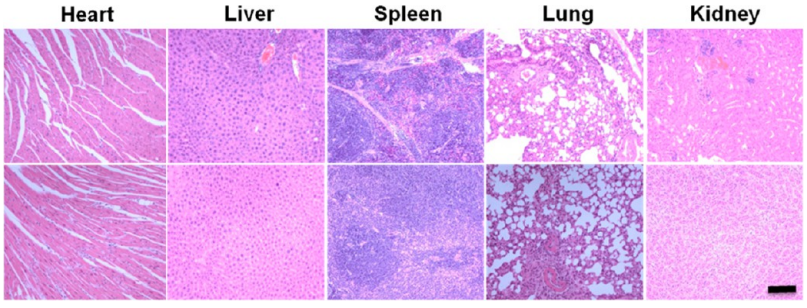

Figure 6. Histopathology of H&E-stained major organs from C57BL/6 mice (top) without treatment and (bottom) after treatment with LCP-(RFP+mc-CR8C)-Gal. Scale bar: 100 μm.

TABLE 3. Hematological Markers of Hepatic and Renal Toxicity as Well as Cytokine Induction[a]

	IL 6 (ng/mL)	IL12 (ng/mL)	IFN (ng/mL)	TNF (ng/mL)	AST (U/L)	ALT (U/L)	BUN (mg/dL)
Mice without treatment	0.6 ± 0.05	0.4 ± 0.14	0.8 ± 0.07	0.1 ± 0.08	141 ± 10.8	67 ± 6.0	22 ± 0.8
Mice treated with LCP	1.5 ± 0.13	0.9 ± 0.12	0.8 ± 0.02	2.2 ± 0.34	147 ± 8.0	65 ± 2.8	18 ± 1.0
95% CI	-	-	-	-	43 - 397	27 - 195	5 - 26

[a] Data are reported as mean ± SD; 95% CI were derived from the technical data sheet C57BL/6 Mouse Hematology (North American Colonies, January 2008 to December 2011), Charles River Laboratories (Wilmington, MA).

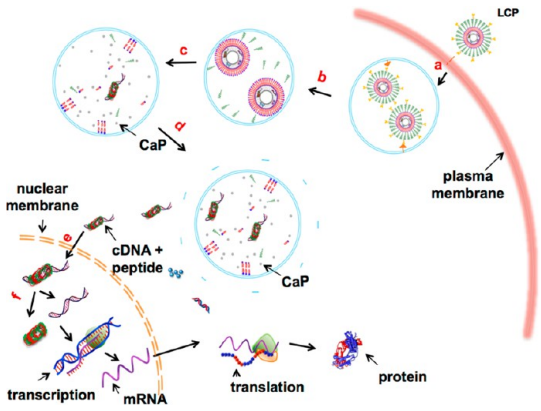

Scheme 1. Proposed mechanism for intracellular delivery of DNA by LCP. (a) ASGPR-mediated endocytosis, elicited by binding to galactose ligands on LCP, supports internalization into hepatocytes. (b) PEGylation shedding is driven by a decrease in endosomal pH.[37] (c) Dissolution of the calcium phosphate core and breakdown of the lipid membrane promotes (d) disruption of the endosome in a cationic lipid-mediated manner. (e) Nuclear import of DNA is thought to be mediated by cysteine-flanked octaarginine peptides. (f) DNA is released in the nucleus for active transcription

Multifunctional Envelope-Type Nanodevices (MEND) delivery system, which elicited hepatic luciferase activity of appx. 1.3×10^6 RLU/mg protein after intravenous injection at 2.5 mg DNA/kg.[10] Scaling linearly for activity and dose, targeted mc-CR8C-containing LCP likely outperforms MEND by roughly 300-fold. Certain design aspects of LCP likely prove beneficial over MEND-type nanoparticles. The smaller size of LCP (55 nm, *vs* 185 nm for the optimized R8-GALA-MEND) may allow for easier penetration through the hepatic sinusoidal fenestrations, allowing increased formulation exposure on a per-cell basis. Intracellular release from PEI, the DNA condensing agent in the MEND formulation, may be limited in comparison to calcium phosphate core degradation.[35] The high intracellular calcium conditions produced by our formulation may aid in endosomal release as well.[50] Further, establishing the octaarginine peptide within the nanoparticle core may better promote DNA delivery on a post-endosomal basis.

Systemic toxicity and cytokine induction of LCP was investigated 24 h after intravenous administration to C57BL/6 mice as well. There were no obvious histological differences between the major organs of treated and untreated mice (Figure 6), and hematological markers remained relatively unperturbed; however, a notable increase in TNF-α was observed (Table 3). Further analysis will be required to determine the significance, if any, of such a response.

CONCLUSIONS

We have developed membrane-core LCP nanoparticles that address a variety of the needs in DNA delivery, integrating together DOPA-coated CaP cores, octaarginine peptides, cationic and PEGylated lipids, and galactose targeting ligands to achieve high levels of gene expression *in vivo* (Scheme 1). The strength and stability of such cores under physiological conditions confer the desired protection against degradation in circulation while supporting both an asymmetric and a highly functionalized lipid bilayer. Such a formulation can efficiently encapsulate DNA as a relatively small vector which presents as ideal in size and PEGylation for delivery to hepatocytes *in vivo*. Further, ASGPR-targeting *via* galactose supports increased and rapid distribution to the liver, presumably through an increased rate of internalization of LCP. Such particles have shown to be effective in cytosolic release of DNA, and co-delivery with the cationic peptides CR8C supports extensive nuclear translocation in post-mitotic cells, with favorable release from mc-CR8C likely contributing to enhanced efficacy over l-CR8C. Gene expression still limits nonviral efforts,[51] as can be observed by comparison to hydrodynamic injection; however, this formulation presents as a much less invasive alternative and, to our knowledge, it is the most effective synthetic vector for liver gene transfer.

MATERIALS AND METHODS

1,2-Distearoyl-*sn*-glycero-3-phosphatidylethanolamine-*N*-[succinyl(polyethylene glycol)-2000]-*N*-hydroxysuccinimide (DSPE-PEG_{2000}−*N*-hydroxysuccinimide (NHS)) was purchased from NOF Corporation (Tokyo, Japan). Radioactive $^{111}InCl_3$ in 0.05 N HCl was purchased from PerkinElmer, Inc. and utilized immediately upon receipt. DSPE-PEG_{2000}-galactose was synthesized through the conjugation of 10 equiv of 4-aminophenyl β-D-galactopyranoside and 1 equiv of DSPE-PEG_{2000}-NHS in PBS buffer, followed by chloroform extraction and dialysis against water using a MWCO 1000 dialysis tube. All other lipids were purchased from Avanti Polar Lipids, Inc. (Alabaster, AL). Peptides were purchased from Elim Biopharmaceuticals, Inc. (Hayward, CA); monocyclic abbreviated to mc, linear abbreviated to l. FAM and Cy3 labeling kits were purchased from Mirus Bio LLC. (Madison, WI). SYBR Green I nucleic acid gel stain (S7585) was purchased from Invitrogen (Grand Island, NY). Luciferin was purchased from Promega Corporation (Madison, WI). Plasmids encoding tdTomato red fluorescence protein (RFP) or firefly luciferase (Luc) driven by the cytomegalovirus promoter were custom prepared by Bayou Biolabs (Harahan, LA). All other chemicals were obtained from Sigma-Aldrich (St. Louis, MO) and used without further purification.

Six-week-old C57BL/6 female mice (~18 g each) were purchased from Charles River Laboratories (Wilmington, MA). All work performed on animals was in accordance with and approved by the University of North Carolina Institutional Animal Care and Use Committee.

Methods. *Preparation and Characterization of LCP Loaded with DNA.* LCP was prepared using a modified protocol.[35] Two separate microemulsions (20 mL each) were prepared of Igepal 520 and cyclohexane (3:7 v/v) and placed under stirring. DNA (60 μg) was added to 600 μL of 2.5 M $CaCl_2$, whose pH had been titrated above 7 with NaOH. To this solution, octaarginine peptides were added at an N:P ratio of 2:1. A Na_2HPO_4 solution (600 μL, 12.5 mM, pH 9) was also prepared, as was 250 μL of

20 mM DOPA (in $CHCl_3$). To one emulsion, the calcium phase was added, while to the other, both the phosphate solution and DOPA were added; both emulsions were left to stir for 20 min. The emulsions were then mixed, and left to stir an additional 20 min. An equal volume of 100% EtOH was added to disrupt the emulsion, and the mixture was centrifuged at 10 000*g* for 20 min. After decanting the supernatant, the precipitate was washed twice thereafter with 100% EtOH to remove traces of Igepal and/or cyclohexane. The precipitate was then dried under N_2, and resuspended in $CHCl_3$. This solution was centrifuged at 6000 rpm for 5 min for the removal of large aggregates, and the supernatant containing the LCP "cores" (DNA and peptide entrapped within a calcium phosphate nanoprecipitate, supporting and surrounded by a lipid monolayer of DOPA) was recovered.

To characterize DNA entrapment efficiency, firefly luciferase cDNA was labeled with Cy3 (Mirus *LabelIT* kit, Mirus Bio, Madison, WI) according to manufacturer instructions. Such Cy3-DNA was formulated into the LCP cores, after which recovery was assessed *via* fluorescence spectrometry. ^{111}In-labeled LCP cores were prepared as described previously,[36] with the addition of $^{111}InCl_3$ into the $CaCl_2$ solution of the calcium emulsion. Upon coprecipitation of the two emulsions, ^{111}In-labeled LCP cores were collected as described above, with centrifugation in $CHCl_3$ removing aggregates containing ^{111}In. The final LCP cores encapsulated 85% of ^{111}In.

LCP was produced through desiccation of a mixture of free lipids and cores (2.5:1 ratio of total free lipids to DOPA) and subsequent rehydration. Therein, 35 mol % DOTAP, 35 mol % cholesterol, and 30 mol % DSPE-PEG_{2000} (or 25 mol % DSPE-PEG and 5 mol % DSPE-PEG-Gal) were utilized as outer leaflet lipids. Zeta potential and particle size of LCP were measured using a Malvern ZetaSizer Nano Series (Westborough, MA). TEM images of LCP were acquired using a JEOL 100CX II TEM (JEOL, Japan).

Pharmacokinetics, Biodistribution, and Intracellular Distribution of Cy3-DNA Delivered by LCP. LCP containing Cy3-DNA, both untargeted and targeted *via* galactose ligands (LCP-PEG and LCP-Gal, respectively, 0.2 mg/kg DNA dose), were injected (0.2 mL, balanced in osmolarity with the addition of dextrose) into 6-week-old C57/BL female mice through the tail vein. Liver tissues were frozen in OCT compound for sectioning. Liver sections (10 μm) were fixed with cold acetone, washed in PBS, and incubated for 5 min with fluorescein isothiocyanate (FITC)-labeled phalloidin in PBS. The sections were stained with DAPI prior to mounting with Fluor-mount G (Southern Biotech), and imaged on a Leica SP2 confocal microscope. UV, Cy3, and FITC filters were set up to image nuclei, intracellular DNA distribution, and actin, respectively.

Pharmacokinetics and quantitative biodistribution were further determined *via* coencapsulation with ^{111}In (incorporated into the calcium emulsion during formulation) in the nanoprecipitate. Such methods have been utilized previously to accurately determine LCP biodistribution.[36] Six-week-old C57BL/6 female mice (6 mice utilized for each group) were injected individually (0.2 mL, balanced in osmolarity with the addition of dextrose) with LCP at 0.1 mg DNA/kg, corresponding to a dose of 8×10^6 cpm/kg of ^{111}In. For pharmacokinetic analysis, blood was recovered at various time points (20, 90, 200, 390, 480, 600, and 720 min) *via* retro-orbital bleed. For biodistribution analysis, 6 and 12 h after the administration of LCP, the blood and major organs were collected (6 mice utilized for each time point). Radioactivity in the blood and tissues in both studies was measured using a γ-counter. Analysis was conducted under a two-compartment model utilizing Phoenix WinNonlin (Version 6.3, Pharsight Corporation; Mountain View, CA).

In Vivo Gene Expression. Several groups of LCPs containing cDNA encoding tdTomato red fluorescence protein (RFP) or firefly luciferase (Luc) were injected (0.2 mL, balanced in osmolarity with the addition of dextrose) into 6-week-old C57BL/6 female mice (0.3 mg DNA/kg, 3 mice utilized for each group) through the tail vein. Hydrodynamic injection was conducted by rapid injection of a 1.6 mL solution of equal DNA dose in PBS. The major organs of the RFP-transfected mice were harvested 24 h postinjection and visualized using a Kodak *in vivo* imaging system FX Pro (Kodak, Rochester, NY) at ex/em = 550/600 nm. For quantitative analysis of gene expression *via* luciferase activity, lysis buffer (0.1 M Tris-HCl, 2 mm EDTA, 0.1% Triton X-100, pH 7.8) was added to each whole organ (1 mL per kidney, spleen, lung, or heart; 15 mL per liver). Each organ was homogenized for 30 s, and homogenates were then centrifuged at 4 °C for 10 min at 13 000*g*. Total protein concentration in the lysate was determined through a bicinchoninic acid protein assay kit (BCA Protein Assay Kit, Pierce, Rockford, IL). Ten microliters of each homogenate supernatant was mixed with 90 μL of luciferase assay reagent (Luciferase Assay System, Promega Co., Madison, WI) and the luminescence intensity was measured *via* plate reader (Bioscan, Inc., Washington, DC) for 1 s. The activity of luciferase is shown as the luminescence intensity per milligram of protein.

DNA Condensation and Release from CR8C. DNA condensation refers to an inhibition of the DNA-intercalated SYBR green fluorescence signal in the presence of either l-CR8C or mc-CR8C peptides. The assay was carried out in 1.5 mL Eppendorf tubes, where 10 μL of SYBR Green (10 000 dilution from stock) and 10 μL of pDNA (100 ng/μL) in 1 mL of 100 mM Tris-HCl (pH 8.0) were mixed and incubated in the dark for 5 min at room temperature. Twenty microliters of peptide solutions corresponding to different charge ratios was subsequently added, followed by incubation in the dark for 15 min. Two controls were prepared without peptide added. Fluorescence signals were recorded at a 497/520 excitation/emission (fluorescence spectrometer, Perkin-Elmer, Waltham, MA), with the control values taken as maximum (*i.e.*, 100%). The inhibition in fluorescence signal was calculated at increasing charge ratios and plotted as percentage of maximum.

For DNA release, the DNA−peptide complexes (10 μL of 100 ng/μL pDNA in each case) were prepared at a charge ratio 4 and incubated with 10 μL of SYBR Green (10 000 dilution from stock) in 1 mL of 100 mM Tris-HCl buffer (pH 8.0) for 30 min at room temperature. Thirty microliters of hyaluronic acid solution was added to the different tubes of DNA−-peptide complexes with SYBR green at increasing amounts. Three controls (pDNA with SYBR green, SYBR green alone, and hyaluronic acid with SYBR green) were also prepared. The fluorescence was recorded as described in the condensation section. The fluorescence value of pDNA−peptide complexes without any hyaluronic acid was taken as 100%, and the relative percentage increase in fluorescence signal was calculated at increasing concentration of hyaluronic acid solutions in terms of charge ratio over the negative charges of DNA.

Toxicity and Pathology Studies. Twenty-four hours after mice were treated with luciferase DNA and mc-CR8C- loaded LCP (0.4 mg DNA/kg) (three mice utilized for each group), serum was obtained from the mice *via* retro-orbital bleed and centrifugation. Hepatic and renal damage was assessed by measuring the levels of AST, ALT and BUN in the serum samples. These measurements were quantified by the Animal Clinical Chemistry and Gene Expression Laboratories at UNC Chapel Hill. An ELISA assay kit (BD Biosciences, San Diego, CA) was used to perform a cytokine induction assay, providing the IL-6, IL-12, IFN-γ and TNF-α levels in the mouse serum. Further, the major organs of each mouse were collected, fixed, and processed thereafter for H&E staining. Images of tissue sections were collected using a Nikon light microscope with 10× objective. The 95% CI were derived from the technical data sheet *C57BL/6 Mouse Hematology* (North American Colonies, January 2008 to December 2011), Charles River Laboratories (Wilmington, MA).

Statistical Analysis. Statistical analysis in luciferase activity comparisons was conducted using Bonferroni-corrected *t* tests. A $p < 0.0125$ was considered significant.

Conflict of Interest: The authors declare no competing financial interest.

Acknowledgment. This work was supported by NIH grants CA129835, CA149363, CA125273 and CA151652. K. Racette helped to edit the manuscript and B. DiPrete helped to draw the scheme.

Supporting Information Available: CR8C mass spectra, *in vitro* cell uptake results, and intracellular DNA distribution profiles. This material is available free of charge *via* the Internet at http://pubs.acs.org.

REFERENCES AND NOTES

1. Niidome, T.; Huang, L. Gene Therapy Progress and Prospects: Nonviral Vectors. *Gene Ther.* **2002**, *9*, 1647–1652.
2. Douglas, K. L. Toward Development of Artificial Viruses for Gene Therapy: A Comparative Evaluation of Viral and Nonviral Transfection. *Biotechnol. Prog.* **2008**, *24*, 871–883.
3. Roth, C. M.; Sundaram, S. Engineering Synthetic Vectors for Improved DNA Delivery: Insights from Intracellular Pathways. *Annu. Rev. Biomed. Eng.* **2004**, *6*, 397–426.
4. Mastrobattista, E.; van der Aa, M. A. E. M.; Hennink, W. E.; Crommelin, D. J. A. Artificial Viruses: A Nanotechnological Approach to Gene Delivery. *Nat. Rev. Drug Discovery* **2006**, *5*, 115–121.
5. Poelstra, K.; Prakash, J.; Beljaars, L. Drug Targeting to the Diseased Liver. *J. Controlled Release* **2012**, *161*, 188–197.
6. Muller, K.; Nahde, T.; Fahr, A.; Muller, R.; Brusselbach, S. Highly Efficient Transduction of Endothelial Cells by Targeted Artificial Virus-like Particles. *Cancer Gene Ther.* **2001**, *8*, 107–117.
7. Mastrobattista, E.; Kapel, R. H. G.; Eggenhuisen, M. H.; Roholl, P. J. M.; Crommelin, D. J. A.; Hennink, W. E.; Storm, G. Lipid-coated Polyplexes for Targeted Gene Delivery to Ovarian Carcinoma Cells. *Cancer Gene Ther.* **2001**, *8*, 405–413.
8. Rozema, D. B.; Lewis, D. L.; Wakefield, D. H.; Wong, S. C.; Klein, J. J.; Roesch, P. L.; Bertin, S. L.; Reppen, T. W.; Chu, Q.; Blokhin, A. V.; *et al.* Dynamic PolyConjugates for Targeted *in Vivo* Delivery of siRNA to Hepatocytes. *Proc. Natl. Acad. Sci. U.S.A.* **2007**, *104*, 12982–12987.
9. Van den Bossche, J.; Al-Jamal, W. T.; Yilmazer, A.; Bizzarri, E.; Tian, B. W.; Kostarelos, K. Intracellular Trafficking and Gene Expression of pH-Sensitive, Artificially Enveloped Adenoviruses *in Vitro* and *in Vivo*. *Biomaterials* **2011**, *32*, 3085–3093.
10. Khalil, I. A.; Hayashi, Y.; Mizuno, R.; Harashima, H. Octaarginine- and pH-Sensitive Fusogenic Peptide-Modified Nanoparticles for Liver Gene Delivery. *J. Controlled Release* **2011**, *156*, 374–380.
11. Peluffo, H.; Aris, A.; Acarin, L.; Gonzalez, B.; Villaverde, A.; Castellano, B. Nonviral Gene Delivery to the Central Nervous System Based on a Novel Integrin-Targeting Multifunctional Protein. *Hum. Gene Ther.* **2003**, *14*, 1215–1223.
12. Aris, A.; Villaverde, A. Modular Protein Engineering for Non-Viral Gene Therapy. *Trends Biotechnol.* **2004**, *22*, 371–377.
13. Akinc, A.; Zumbuehl, A.; Goldberg, M.; Leshchiner, E. S.; Busini, V.; Hossain, N.; Bacallado, S. A.; Nguyen, D. N.; Fuller, J.; Alvarez, R.; *et al.* A Combinatorial Library of Lipid-like Materials for Delivery of RNAi Therapeutics. *Nat. Biotechnol.* **2008**, *26*, 561–569.
14. Love, K. T.; Mahon, K. P.; Levins, C. G.; Whitehead, K. A.; Querbes, W.; Dorkin, J. R.; Qin, J.; Cantley, W.; Qin, L. L.; Racie, T.; *et al.* Lipid-like Materials for Low-Dose, *in Vivo* Gene Silencing. *Proc. Natl. Acad. Sci. U.S.A.* **2010**, *107*, 1864–1869.
15. Ojea-Jiménez, I.; García-Fernández, L.; Lorenzo, J.; Puntes, V. F. Facile Preparation of Cationic Gold Nanoparticle-Bioconjugates for Cell Penetration and Nuclear Targeting. *ACS Nano* **2012**, *6*, 7692–7702.
16. Ashley, C. E.; Carnes, E. C.; Epler, K. E.; Padilla, D. P.; Phillips, G. K.; Castillo, R. E.; Wilkinson, D. C.; Wilkinson, B. S.; Burgard, C. A.; Kalinich, R. M.; *et al.* Delivery of Small Interfering RNA by Peptide-Targeted Mesoporous Silica Nanoparticle-Supported Lipid Bilayers. *ACS Nano* **2012**, *6*, 2174–2188.
17. Khalil, I. A.; Kogure, K.; Futaki, S.; Hama, S.; Akita, H.; Ueno, M.; Kishida, H.; Kudoh, M.; Mishina, Y.; Kataoka, K.; et al. Octaarginine-modified Multifunctional Envelope-Type Nanoparticles for Gene Delivery. *Gene Ther.* **2007**, *14*, 682–689.
18. *Schiff's Diseases of the Liver*, 11th ed.; Schiff, E. R.; Maddrey, W. C.; Sorrell, M. F., Eds.; John Wiley and Sons, Ltd.: Oxford; 2012.
19. Schilsky, M. Wilson Disease: New Insights into Pathogenesis, Diagnosis, and Future Therapy. *Curr. Gastroenterol. Rep.* **2005**, *7*, 26–31.
20. Flotte, T. R.; Mueller, C. Gene Therapy for Alpha-1 Antitrypsin Deficiency. *Hum. Mol. Genet.* **2011**, *20*, R87–R92.
21. Perry, D. J. Factor VII Deficiency. *Br. J. Hamaetol.* **2002**, *118*, 689–700.
22. Snoeys, J.; Lievens, J.; Wisse, E.; Jacobs, F.; Duimel, H.; Collen, D.; Frederik, P.; De Geest, B. Species Differences in Transgene DNA Uptake in Hepatocytes after Adenoviral Transfer Correlate with the Size of Endothelial Fenestrae. *Gene Ther.* **2007**, *14*, 604–612.
23. Crispe, I. N. Hepatic T Cells and Liver Tolerance. *Nat. Rev. Immunol.* **2003**, *3*, 51–62.
24. Rensen, P. C.; Sliedregt, L. A.; Ferns, M.; Kieviet, E.; van Rossenberg, S. M.; van Leeuwen, S. H.; van Berkel, T. J.; Biessen, E. A. Determination of the Upper Size Limit for Uptake and Processing of Ligands by the Asialoglycoprotein Receptor on Hepatocytes *in Vitro* and *in Vivo*. *J. Biol. Chem.* **2001**, *276*, 37577–37584.
25. Zhang, X. Q.; Wang, X. L.; Zhang, P. C.; Liu, Z. L.; Zhuo, R. X.; Mao, H. Q.; Leong, K. W. Galactosylated Ternary DNA/Polyphosphoramidate Nanoparticles Mediate High Gene Transfection Efficiency in Hepatocytes. *J. Controlled Release* **2005**, *102*, 749–763.
26. Sonawane, N. D.; Szoka, F. C., Jr.; Verkman, A. S. Chloride Accumulation and Swelling in Endosomes Enhances DNA Transfer by Polyamine-DNA Polyplexes. *J. Biol. Chem.* **2003**, *278*, 44826–44831.
27. Hafez, I. M.; Maurer, N.; Cullis, P. R. On the Mechanism whereby Cationic Lipids Promote Intracellular Delivery of Polynucleic Acids. *Gene Ther.* **2001**, *8*, 1188–1196.
28. Lee, S.; Yang, S. C.; Kao, C.-Y.; Pierce, R. H.; Murthy, N. Solid Polymeric Microparticles Enhance the Delivery of siRNA to Macrophages *in Vivo*. *Nucleic Acids Res.* **2009**, *37*, e145.
29. McKenzie, D. L.; Smiley, E.; Kwok, K. Y.; Rice, K. G. Low Molecular Weight Disulfide Cross-Linking Peptides as Nonviral Gene Delivery Carriers. *Bioconjugate Chem.* **2000**, *11*, 901–909.
30. Kim, T.-i.; Ou, M.; Lee, M.; Kim, S. W. Arginine-Grafted Bioreducible Poly(disulfide amine) for Gene Delivery Systems. *Biomaterials* **2009**, *30*, 658–664.
31. Gao, Y.; Xu, Z.; Chen, S.; Gu, W.; Chen, L.; Li, Y. Arginine-Chitosan/DNA Self-Assembled Nanoparticles for Gene Delivery: *In Vitro* Characteristics and Transfection Efficiency. *Int. J. Pharm.* **2008**, *359*, 241–246.
32. Manickam, D. S.; Oupický, D. Multiblock Reducible Copolypeptides Containing Histidine-Rich and Nuclear Localization Sequences for Gene Delivery. *Bioconjugate Chem.* **2006**, *17*, 1395–1403.
33. Won, Y.-W.; Kim, H. A.; Lee, M.; Kim, Y.-H. Reducible Poly(oligo-D-arginine) for Enhanced Gene Expression in Mouse Lung by Intratracheal Injection. *Mol. Ther.* **2010**, *18*, 734–742.
34. Melikov, K.; Chernomordik, L. V. Arginine-Rich Cell Penetrating Peptides: from Endosomal Uptake to Nuclear Delivery. *Cell. Mol. Life Sci.* **2005**, *62*, 2739–2749.
35. Li, J.; Yang, Y.; Huang, L. Calcium Phosphate Nanoparticles with an Asymmetric Lipid Bilayer Coating for siRNA Delivery to the Tumor. *J. Controlled Release* **2012**, *158*, 108–114.
36. Liu, Y.; Tseng, Y.-c.; Huang, L. Biodistribution Studies of Nanoparticles Using Fluorescence Imaging: A Qualitative or Quantitative Method? *Pharm. Res.* **2012**, *29*, 3273–3277.
37. Huang, L.; Liu, Y. *In Vivo* Delivery of RNAi with Lipid-Based Nanoparticles. *Annu. Rev. Biomed. Eng.* **2011**, *13*, 507–530.
38. Mudhakir, D.; Harashima, H. Learning from the Viral Journey: How To Enter Cells and How To Overcome Intracellular Barriers To Reach the Nucleus. *AAPS J.* **2009**, *11*, 65–77.
39. Torchilin, V. P. Tat Peptide-Mediated Intracellular Delivery of Pharmaceutical Nanocarriers. *Adv. Drug Delivery Rev.* **2008**, *60*, 548–558.
40. Nakase, I.; Takeuchi, T.; Tanaka, G.; Futaki, S. Methodological and Cellular Aspects that Govern the Internalization Mechanisms of Arginine-Rich Cell-Penetrating Peptides. *Adv. Drug Delivery Rev.* **2008**, *60*, 598–607.
41. Pan, L.; He, Q.; Liu, J.; Chen, Y.; Ma, M.; Zhang, L.; Shi, J. Nuclear-Targeted Drug Delivery of TAT Peptide-Conjugated Monodisperse Mesoporous Silica Nanoparticles. *J. Am. Chem. Soc.* **2012**, *134*, 5722–5725.

42. Liu, Y.; Nieh, M. P.; Heller, W.; Hu, Y.; Huang, L. Nanoparticle Delivery to Hepatocytes Requires a Compact, Non-Brush Conformation of the Polyethylene Glycol Coating. *Drug Carriers in Medicine and Biology*; Gordon Research Conferences: Waterville Valley, NH; 2012.
43. Liu, F.; Song, Y. K.; Liu, D. Hydrodynamics-Based Transfection in Animals by Systemic Administration of Plasmid DNA. *Gene Ther.* **1999**, *6*, 1258–1266.
44. Grigsby, C. L.; Leong, K. W. Balancing Protection and Release of DNA: Tools to Address a Bottleneck of Non-Viral Gene Delivery. *J. R. Soc. Interface* **2010**, *7*, S67–S82.
45. Mann, A.; Thakur, G.; Shukla, V.; Singh, A. K.; Khanduri, R.; Naik, R.; Jiang, Y.; Kalra, N.; Dwarakanath, B. S.; Langel, U.; *et al.* Differences in DNA Condensation and Release by Lysine and Arginine Homopeptides Govern Their DNA Delivery Efficiencies. *Mol. Pharmaceutics* **2011**, *8*, 1729–1741.
46. Liu, J.; Jiang, Z.; Zhou, J.; Zhang, S.; Saltzman, W. M. Enzyme-synthesized Poly(amine-co-esters) as Nonviral Vectors for Gene Delivery. *J. Biomed. Mater. Res. A.* **2011**, *96A*, 456–465.
47. Kim, K. S.; Lei, Y.; Stolz, D. B.; Liu, D. Bifunctional Compounds for Targeted Hepatic Gene Delivery. *Gene Ther.* **2007**, *14*, 704–708.
48. Gao, Y.; Yin, Q.; Chen, L.; Zhang, Z.; Li, Y. Linear Cationic Click Polymers/DNA Nanoparticles: In Vitro Structure −Activity Relationship and In Vivo Evaluation for Gene Delivery. *Bioconjugate Chem.* **2011**, *22*, 1153–1161.
49. Fortune, J. A.; Novobrantseva, T. I.; Klibanov, A. M. Highly Effective Gene Transfection In Vivo by Alkylated Polyethylenimine. *J. Drug Delivery* **2011**, 6.
50. Fujita, T.; Furuhata, M.; Hattori, Y.; Kawakami, H.; Toma, K.; Maitani, Y. Calcium Enhanced Delivery of Tetraarginine-PEG-Lipid-Coated DNA/Protamine Complexes. *Int. J. Pharm.* **2009**, *368*, 186–192.
51. Kogure, K.; Akita, H.; Yamada, Y.; Harashima, H. Multifunctional Envelope-Type Nano Device (MEND) as a Non-viral Gene Delivery System. *Adv. Drug Delivery Rev.* **2008**, *60*, 559–571.